

SĀDHANĀ

Volume 39

Number 6
(200)

2014

- 1259 **Varun Krishna · Jintomon Jose · N N R Ranga Suri**
Design and development of a web-enabled data mining system employing JEE technologies
- 1271 **S C Dutta Roy**
Some recent work on lattice structures for digital signal processing
- 1295 **Vikas Kumar · Prerna Gaur · A P Mittal**
High performance predictive current control of a three phase VSI: An experimental assessment
- 1311 **Sartajvir Singh · Rajneesh Talwar**
A comparative study on change vector analysis based change detection techniques
- 1333 **G Raju · Bindu S Momi · Madhu S Nair**
A novel handwritten character recognition system using gradient based features and run length count
- 1357 **Rishabh Iyer · Rushikesh Borse · Subhasis Chaudhuri**
Embedding capacity estimation of reversible watermarking schemes
- 1387 **M Vasudevan · G Suresh Kumar · Indumathi M Nambi**
Numerical modelling of multicomponent LNAPL dissolution kinetics at residual saturation in a saturated subsurface system
- 1409 **Sunil Kumar Kopparapu · Vikram Saxena**
Identifying the best market to sell: A cost function formulation

(continued on inside back cover)

Indexed in: Current Contents

Edited and published by R Ramaswamy for the Indian Academy of Sciences, Bangalore 560 080.
Printed at Brilliant Printers Pvt. Ltd, Bangalore 560 094.

Registered with Registrar of Newspapers in India, vide Regn No. 13242/57

₹ 40 ISSN 0256-2499

Volume 39 · Number 6 · December 2014

SĀDHANĀ

Academy Proceedings in Engineering Sciences

12046

■ SĀDHANĀ



Indian Academy
of Sciences

 Springer

Exploring the electrodes alignment and mushrooming effects on weld geometry of dissimilar steels during the spot welding process

NACHIMANI CHARDE

¹Department of Mechanical, Material and Manufacturing Engineering,
The University of Nottingham Malaysia Campus, Jalan Broga,
43500 Semenyih, Selangor Darul Ehsan, Malaysia

²Department of Mechanical Engineering, Faculty of Engineering, University of
Malaya, 50603 Kuala Lumpur, Malaysia
e-mail: nachi.charde@nottingham.edu.my;nachimani@um.edu.my

MS received 18 March 2013; revised 12 June 2014; accepted 7 August 2014

Abstract. The class two of RWMA electrode caps has very common application-purpose for the welding of steels and withstand for high thermal application on wrought cast. It has been experimentally used to weld carbon and stainless steels up to 900 weld attempts using AC waveform, C-type JPC 75 kVA, Japanese made spot welder. So the electrode alignments and resulting mushrooming effects are finally analysed in this research as well as the weld geometry of dissimilar (carbon and stainless) steels. When considering such weld joints, the heat imbalances are very interesting factors on spot welding research and therefore I have simulated the dissimilar weld joints using Ansys 14. Initially, it was simulated and later those results are compared with real welded samples. The common welded regions such as: fusion zones, heat affected zones, heat extended zones and base metals are all well-noticed for carbon steel sides but not for stainless steel sides. Besides, the electrode mushrooming effect on both sides of electrodes are not parallel deterioration and it has some demerits on internal structure indeed. Some of the dissimilar welded samples and electrode caps are eventually underwent metallurgical test to identify the improper alignment.

Keywords. Spot welding; dissimilar joints; electrode deformation; electrode mushrooming.

1. Introduction

The geometry of dissimilar weld joints is basically made of asymmetrical weld nuggets. In such welding joints, the heat imbalances will be the main factor and it has to be properly aligned in the middle of base metal to produce a proper weld nugget (Aravinthan & Nachimani 2011a). So the electrode alignment during welding process plays a significant role on the formation of weld

geometry. In this research, the carbon and stainless steels are analysed for the weld nuggets alignment as well as the mushrooming growth of electrodes after 900 welds were done. The growth of the weld nugget is therefore determined by the welding current, sufficient time for current delivery, reasonable electrode pressing force and sufficient area for current delivery (electrode tip) (Aravinthan & Nachimani 2011b). Basically, the welding current and weld time lead to the root generation of heat in the welding process while the electrode pressing force and electrode tips' accomplish it successfully (Mehdi *et al* 2008). Although the welding current and weld time cause the heat generation at the concerned areas (electrode tips' area); the electrode tips diameter and electrode pressing forces are also directly influencing the welding process (Nachimani 2012). So the class two electrode types are engaged in the welding process and consequently monitored the deformation and mushrooming effects after approximately 900 welds were done.

2. Experimentation

The carbon and stainless steels were prepared in rectangular shape (Chang *et al* 2006) with a size of the length (200 mm); width (25 mm) and thickness (1 mm). A pair of water cooled (2 liters per minutes) 30 degree truncated type of electrodes (5 mm of diameter) was used to join (JPC 75 kVA) of these base metals as shown in figure 1. The pair of test sample was initially loaded on the top of lower electrode (tip) of the welder as overlaying 60 mm on each other (lap joint) and then the initiating pedal was pressed. The upper electrode lever has moved towards the lower electrode and squeezed the based metals that placed in between (Rao *et al* 2009). The welding current was released immediately after the squeezing cycles of pneumatic based electrode actuation is achieved. Thereafter the electrode pressing mechanism has consumed some time for cold work and eventually returned to the home position of upper electrode (Yeung & Thornton 1999). These process controlling parameters (welding current, weld time and electrode pressing force)

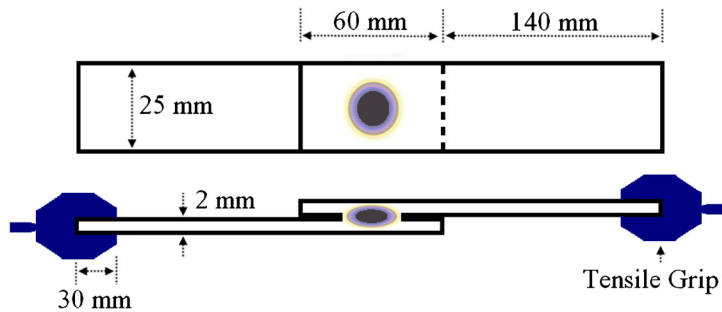


Figure 1. Lap joint welding process.

Table 1. The chemical properties of base metals.

304L (2B) Austenitic stainless steel							
Element	C	Cr	Ni	Mn	Si	S	P
	0.048	18.12	8.11	1.166	0.501	0.006	0.030
Carbon steel							
Element	C	Cr	Ni	Mn	Si	S	P
	0.23			0.90	0.006	0.050	0.040

Table 2. General properties of CMW copper based alloys.

CMW Alloy (Class 2)	CMW 3 (ME 14 Z)
Condition	Cast wrought
Principle elements	Copper, chromium
RWMA alloy number	2.18200
Rockwell hardness (HRB)	70–83 B
Electrical conductivity % IACS	80–85
Ultimate tensile strength (PSI)	55–75 k
Elongation % in 2"	15–20
Permanent softening begin at	500°C



Figure 2. Hot press mounted samples for SEM scanning.

were set before the welding process starts; based on the manufacturers of welding lobe for 1 mm thicknesses. Table 1 lists the chemical properties of base metals and table 2 lists the general description of copper based alloy-electrodes that used in this analysis.

The welded sample was cut at the line of its diameter and mounted using resin powder on hot press mount (Marashi *et al* 2008). The mounted samples (figure 2) were roughly polished using silicon papers 1200/800 p and 600/200 p; and also continuously polished using Metadi polishing cloth with suspension liquid of 0.05 micron. This polishing process has been conducted about thirty minutes to one hour on each sample until the shining surface was seen. At last, the ferric chloride (500 ml) was used to immerse these well-prepared (shining surface) samples in a pot about 30–45 minutes. After that the samples were rinsed off using plain water; dried using air blower; anti-corrosion liquid was applied and kept in vacuum chamber for SEM scanning. Similar procedures were carried out to analyse the macro and micro structural changes of electrodes after about 900 welds were made in one year.

3. Results and discussion

3.1 A comparative study of simulation and real type of dissimilar weld joint

A simulation of dissimilar (carbon and stainless steel) weld joint was carried out prior to the real experiment using Ansys 14 (figure 3). The simulation results have revealed asymmetrical fusion zones due to dissimilar thermal characteristics for dissimilar weld joint. So in overall, I have categorized those regions as (i) fusion zone, (ii) heat affected zone, (iii) heat extended zone and (iv) base metal. So it is obvious that the heat imbalances were noticed due to different electrical properties of base metals.

Table 3 lists the general properties of carbon and stainless steels. From table 1, it is clearly seen that the melting point of both metals vary from each other so the melting process starts